PPh_3 occupies the fourth coordination site rather than an exodentate TT[9]OB molecule.[7] Table VIII lists the torsional angles in TT[9]OB for these different $[Ag(TT[9]OB)_2]^+$ cations. Although there are some differences in the chelate ring conformations (δ versus λ), three basic ligand conformations can be distinguished for TT[9]OB: S_3 exo or exodentate, as observed in the free ligand; S_3 endo or endodentate, as found for facial coordination; and S_2 endo/S exo, the conformation which results in bidentate coordination.

Summary and Conclusions

Solution behavior and solid-state structures of the complexes $[Ag(TT[9]OB)_2][X]$ demonstrate that TT[9]OB is capable of easily converting from an exodentate to an endodentate conformation. This property can be attributed to the strain introduced into the free ligand as a result of the incorporation of a rigid *o*-xylyl group. This results in a number of significant observations. (1) Similar to 9S3, TT[9]OB is capable of enforcing octahedral coordination at Ag(I) by sandwiching the ion between two capping ligands. This occurs even though the sulfur donors are not preorganized as in 9S3. (2) TT[9]OB can adopt three different coordination modes and act as a two-, four-, or six-electron donor ligand bonding through one, two, or three sulfur atoms. This combination of apparently strong metal-ligand interaction and conformational flexibility makes TT[9]OB unique in crown thioether chemistry.

Acknowledgment. We thank the Natural Sciences and Engineering Research Council of Canada and the donors of the Petroleum Research Fund, administered by the American Chemical Society, for financial support of this research.

Supplementary Material Available: Listings of crystallographic data collection parameters, positional parameters, thermal parameters, nonessential bond distances and angles, and hydrogen atom parameters (Table S-I-S-XIII) (12 pages); listings of observed and calculated structure factors (Table S-XIV-S-XVI) (22 pages). Ordering information is given on any current masthead page.

Contribution from the Department of Chemistry, Clark University, Worcester, Massachusetts 01610, Department of Chemistry, University of New Hampshire, Durham, New Hampshire 03824, and Chemistry Division, National Research Council of Canada, Ottawa, Canada K1A 0R9

Halogenated Derivatives of the Dimolybdenum Tetraphosphoxane Cage

Mark M. Turnbull,*,† Carmen Valdez,‡ Edward H. Wong,*,‡ Eric J. Gabe,§ and Florence L. Lee§

Received June 16, 1991

Iodination and chlorination of the dimolybdenum tetraphosphoxane cage complex $(CO)_4Mo[^iPr_2NPO]_4Mo(CO)_4$ in dichloromethane afforded first the mixed-valent products $X_2(CO)_2Mo[^iPr_2NPO]_4Mo(CO)_4$ and then the tetrahalo complexes $X_2(CO)_2Mo[^iPr_2NPO]_4Mo(CO)_2X_2$ (X = Cl, I). The tetrabromo complex can be similarly synthesized, but the dibromo complex is not formed by stoichiometric bromination in CH_2Cl_2. It was indirectly prepared by metathesis from the diiodo product in $CH_2Cl_2/CH_3C{\equiv}N$. The integrity of the adamantane-like $Mo_2P_4O_4$ cage is maintained in all these halogenation products. For the cage-I_2 complex, an intermediate species, $I_2(CO)_3Mo[^iPr_2NPO]_4Mo(CO)_4$, can be observed at low temperature. This readily decarbonylates to give the isolated product. A single-crystal X-ray structural determination of the diiodo complex, $I_2(CO)_2Mo[^iPr_2NPO]_4Mo(CO)_4$, has been completed. Crystal data: monoclinic, $P2_1/c$, a = 18.915 (2) Å, b = 11.911 (2) Å, c = 21.063 (2) Å, β = 94.88 (1)°, V = 4728.4 (9) Å^3, Z = 4, D_{calc} = 1.610 g/cm^3, μ = 19.8 cm^{-1}, $F(000)$ = 1919.51, Mo Kα (λ = 0.709 30 Å), R_F = 0.058, and R_w = 0.049 for 4029 unique observed [$|F| \geq 2.5\sigma(F)$] reflections and 468 parameters. A trigonal-prismatic coordination sphere is found around the 16-electron Mo(II) center. NMR spectroscopic data support the retention of this geometry for all the dihalogenated and tetrahalogenated species in solutions of nonpolar solvents. By contrast to these stable products, halogenation of the phenyl-substituted cage complex, $(CO)_4Mo[PhPO]_4Mo(CO)_4$, afforded $X_2(CO)_3Mo[PhPO]_4Mo(CO)_4$ and $X_2(CO)_3Mo[PhPO]_4Mo(CO)_3X_2$. These complexes show low stability, lose CO readily, and are only poorly characterized.

Introduction

One of the most fundamental reaction types of group VI transition-metal diphosphine carbonyl complexes is that with elemental halogens.[1] Typically halogen oxidation of the zerovalent metal to 2+ is accompanied by coordination of two halides as well as loss of one or more carbon monoxide ligands. This is sometimes called an oxidative-elimination reaction. Often, stereochemically nonrigid seven-coordinate complexes of the type $M(CO)_3(PR_3)_2X_2$ are isolated.[2] Structural work on these have revealed capped octahedral as well as pentagonal-bipyramidal geometries for these 18-electron species. Depending on the phosphine ligands and halides, reversible CO loss to generate six-coordinate $M(CO)_2(PR_3)_2X_2$ complexes can also occur.[3] These and related Mo(II) and W(II) complexes without phosphine ligands are formally electron deficient with only 16 metal valence electrons, and substantial structural departures from the preeminent octahedral stereochemistry can be expected due to a first-order Jahn-Teller effect.[4] This is especially prevalent in the presence of π-donating ligands. Thus the molecular structure of $Mo(CO)_2[S_2CN^iPr_2]_2$ is trigonal prismatic, while $Mo(O\text{-}^tBu)_2(CO)_2Py_2$ has a bicapped tetrahedral coordination sphere.[5] Halides can also be expected to function as π donors in the 16-electron $M(CO)_2(PR_3)_2X_2$ family of complexes. Indeed, $Mo(PPh_3)_2(CO)_2Br_2$ has been shown to distort toward a bicapped tetrahedral geometry.[6] By contrast, chelating diphosphines have so far yielded exclusively electron-precise seven-coordinate $Mo(CO)_3$(diphosphine)X_2 products.[7] We have been investigating the halogenation reactions of the dimolybdenum octacarbonyl *cyclo*-tetraphosphoxane complexes $(CO)_4Mo[^iPr_2NPO]_4Mo(CO)_4$ (**1**) and $(CO)_4Mo[PhPO]_4Mo(CO)_4$ (**2**), both of which feature two $Mo(CO)_4$(diphosphine) centers constrained in an adamantanoid cage structure.[8] We are interested in the resulting stereochemistry at the Mo(II) centers,

† Clark University.
‡ University of New Hampshire.
§ National Research Council of Canada.

(1) Early examples include: (a) Cook, C. D.; Nyholm, R. S.; Tobe, M. L. *J. Chem. Soc.* **1965**, 4194. (b) Lewis, J.; Whyman, R. *J. Chem. Soc.* **1965**, 5486. (c) Colton, R.; Rix, C. J. *Aust. J. Chem.* **1969**, *22*, 305.
(2) Colton, R.; Kevekordes, J. *Aust. J. Chem.* **1982**, *35*, 895.
(3) Colton, R.; Scollary, G. R.; Tomkins, I. B. *Aust. J. Chem.* **1968**, *21*, 15.
(4) (a) Kubacek, P.; Hoffmann, R. *J. Am. Chem. Soc.* **1981**, *103*, 4320. (b) Templeton, J. L.; Winston, P. B.; Ward, B. C. *J. Am. Chem. Soc.* **1981**, *103*, 7713.
(5) (a) Templeton, J. L.; Ward, B. C. *J. Am. Chem. Soc.* **1980**, *102*, 6568. (b) Chisholm, M. H.; Huffman, J. C.; Kelly, R. L. *J. Am. Chem. Soc.* **1979**, *101*, 7615.
(6) Drew, M. G. B.; Colton, R.; Tomkins, I. B. *Aust. J. Chem.* **1970**, *23*, 2517.
(7) (a) Bradley, F. C.; Wong, E. H.; Gabe, E. J.; Lee, F. L.; LePage, Y. *Polyhedron* **1987**, *5*, 1103. (b) Keppert, D. L. *Inorganic Stereochemistry*; Springer-Verlag: Berlin, 1982; Chapter 11. (c) Drew, M. G. B. *Prog. Inorg. Chem.* **1977**, *23*, 67.
(8) Wong, E. H.; Turnbull, M. M.; Hutchinson, K. D.; Valdez, C.; Gabe, E. J.; Lee, F. L.; Le Page, Y. *J. Am. Chem. Soc.* **1988**, *110*, 8422.

0020-1669/92/1331-0208$03.00/0

Scheme I

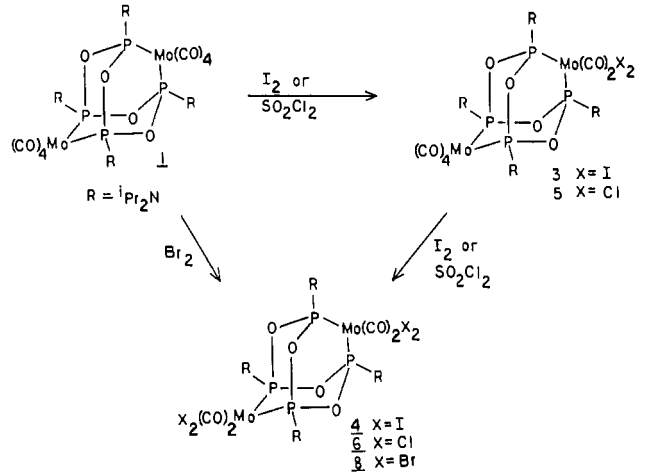

Table I. IR Data for Cage Complexes (cm^{-1})[a]

compd	ν(C≡O)				ν(POP)
1	2015	1923	1906	1887	875 m, d
2	2024	1953	1925		882
3	2024	1979	1915		885 m, d
4		1977	1921		885
5	2025	7975	1960	1920	889 m, d
6		1979	1929		897
7	2024	1979	1953	1909	887 sh, 876
8		1978	1923		890
10	2025	1990	1980	1932	
		1920	1908		897, 882
11	2040	1988	1976	1936	902
12		1992	1927	1886	911
13	2035	1978	1917		897
14		1978	1917		902
15		1988	1931	1883	900
16	2040	1998	1936	1916	902
17	2035	1973	1936		897

[a] In KBr matrix unless otherwise noted; m = medium, sh = shoulder, and d = doublet.

the influence of the P substituents on reactivity, and the existence of mixed-valent cage complexes, as well as evidence for cooperativity effects between the two metal sites.

Results

Halogenation Reactions of $(CO)_4Mo[^iPr_2NPO]_4Mo(CO)_4$. The reaction of **1** with I_2 in dichloromethane solution at room temperature produces the burgundy red, mixed-valent complex $I_2(CO)_2Mo[^iPr_2NPO]_4Mo(CO)_4$ (**3**) in high yield (89%). Further treatment of **3** with I_2 or reaction of **1** with 2 equiv of I_2 yields the symmetrical compound $I_2(CO)_2Mo[^iPr_2NPO]_4Mo(CO)_2I_2$ (**4**) (91%), which is also dark red. Similarly, reaction of **1** with 1 or 2 equiv of SO_2Cl_2 produces the corresponding bright yellow, chloro complexes $Cl_2(CO)_2Mo[^iPr_2NPO]_4Mo(CO)_4$ (**5**) and $Cl_2(CO)_2Mo[^iPr_2NPO]_4Mo(CO)_2Cl_2$ (**6**) in excellent yields (85% and 99%, respectively). In contrast, the reaction of **1** with 1 equiv of Br_2 in dichloromethane solution does not produce the expected mixed-valent complex $Br_2(CO)_2Mo[^iPr_2NPO]_4Mo(CO)_4$ (**7**) but rather the tetrabromo compound $Br_2(CO)_2Mo[^iPr_2NPO]_4Mo(CO)_2Br_2$ (**8**) in 50% yield. An equivalent amount of unreacted **1** is recovered.[9] These results are summarized in Scheme I.

As the mixed-valent bromo complex **7** could not be prepared by direct bromination in CH_2Cl_2, we pursued its synthesis by halide exchange and found that treatment of **3** with a slight excess of $[Et_4N]Br$ in $CH_2Cl_2/CH_3C{\equiv}N$ gave the desired bromide complex **7** in 76% yield (Scheme II).

The identities of compounds **3–8** were confirmed by microanalysis, IR and multinuclear NMR spectroscopy, and, in the case of **3**, single-crystal X-ray diffraction. Relevant IR and NMR data for **3–8** are summarized in Tables I–IV. Crystal data for **3** are given in Table V, along with relevant bond lengths and angles in Table VI.

(9) Preliminary evidence suggests that this reaction is solvent dependent and the monooxidized bromide complex may be formed directly in THF solution: Leslie, D. B., Turnbull, M. M. Unpublished results.

Scheme II

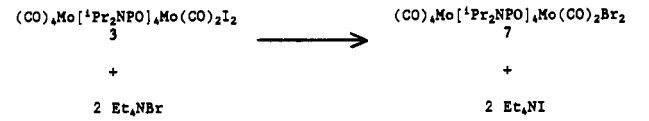

Table II. ^1H NMR[a] Data for **1**, **3–5**, **7**, and **8**

compd	δ
1	4.4 (hept, 1 H, NC*H*), 1.4 (d, 6 H, C*H*$_3$)
3	5.3 (hept, 1 H, NC*H*), 4.05 (hept, 3 H, NC*H*), 1.35 (m, 24 H, C*H*$_3$'s)
4	4.9 (m, 1 H, NC*H*), 3.75 (m, 1 H, NC*H*), 1.40 (app quar, 12 H, CH$_3$)
5	5.3 (m, 1 H, NC*H*), 4.2 (m, 2 H, NC*H*), 3.9 (m, 1 H, NC*H*), 1.45 (d, 6 H, C*H*$_3$), 1.39 (d, 12 H, C*H*$_3$), 1.34 (d, 6 H, C*H*$_3$)
7	5.3 (hept, 1 H, NC*H*), 4.10 (hept, 3 H, NC*H*), 1.35 (m, 24 H, C*H*$_3$)
8[b]	4.9 (m, 1 H, NC*H*), 3.75 (m, 1 H, NC*H*), 1.40 (app quar, 12 H, C*H*$_3$)

[a] Referenced to TMS in $CDCl_3$ solution unless otherwise noted. d = doublet; app quar = apparent quartet; hept = heptet; m = multiplet. [b] In CD_3CN.

Table III. ^{13}C NMR Data[a] for **1**, **3–5**, **7**, and **8**

compd	δ(C≡O)	δ(NCH)	δ(CH$_3$)
1	213.9 (t), 207.3 (t)	47.0 (d)	24.1 (s)
3	233.4 (t), 213.0 (d of d), 211.0 (t), 206.2 (t)	49.0 (t), 48.3 (d), 48.0 (s), 47.0 (s)	24.5 (d), 24.0 (d), 23.2 (s)
4	231.1 (d of d), 229.5 (d of d)	50.6 (d), 49.7 (d)	24.6 (s), 23.1 (m)
5	239.5 (t), 212.8 (t), 212.1 (t), 206.1 (t)	49.5 (t), 48.0 (d), 47.7 (s)	24.7 (s), 24.5 (s), 24.0 (s), 23.3 (s)
7	236.0 (t), 212.8 (d of d), 212.2 (t), 206.3 (t)	49.9 (s), 48.7 (s), 48.5 (s), 48.0 (d)	24.6 (s), 24.1 (s), 23.4 (t)
8[b]	230.4 (m)	49.3 (m)	24.8 (s), 23.2 (m)

[a] In $CDCl_3$ solution unless otherwise noted; s = singlet, d = doublet, t = triplet, and m = multiplet. [b] In CD_3CN.

Table IV. ^{31}P NMR Data[a] for **1–5**, **7**, **8**, and **11–13**

compd	δ[b]
1	150.1 (s)
2	185.2 (s)
3	161.8 (d of t, J_d = 40 Hz, J_t = 2 Hz) 155.4 (d of t, J_d = 40 Hz, J_t = 12 Hz) 132.7 (d of d, J = 12 and 2 Hz)
4[c]	144.7 (d, J = 157 Hz) 137.2 (d, J = 157 Hz)
5	162.9 (d, J = 39 Hz) 157.5 (d of t, J_d = 39, J_t = 15 Hz) 152.0 (d, J = 15 Hz)
7[d]	162.9 (d, J = 40 Hz) 157.5 (d of t, J_d = 40, J_t = 15 Hz) 147.1 (d, J = 15 Hz)
8[e]	157.9 (AA'), AA'BB' pattern 145.1 (BB') (J_{app} = 24, 107 Hz)
11[f]	202.1 (A), ABX_2 pattern 201.7 (B) (J_{AB} = 37 Hz) 152.0 (X) (J_{AX} = J_{BX} = 15 Hz)
12[f]	168 (br)
13[f]	201.9 (A), ABX_2 pattern 200.5 (B) (J_{AB} = 40 Hz) 176.8 (X) (J_{AX} = J_{BX} = 15 Hz)

[a] In $CDCl_3$ solution at 38 MHz unless otherwise noted. [b] Referenced to external 85% H_3PO_4. [c] At 146 MHz. [d] Taken in CD_3CN/CH_2Cl_2 solution. [e] Taken in CD_3CN solution. [f] In CD_2Cl_2 solution at −40 °C.

Table V. Crystallographic Data for $I_2(CO)_2Mo[^iPr_2NPO]_4Mo(CO)_4$ (3)

formula: $C_{30}H_{56}I_2Mo_2N_4O_{10}P_4$	space group: $P2_1/c$
xtal = 0.2 × 0.2 × 0.3 mm	monoclinic, $Z = 4$
fw = 1145.92	$T = 295$ K
$a = 18.915$ (2) Å	$\lambda = 0.709\,30$ Å
$b = 11.911$ (2) Å	$D_{calc} = 1.610$ g/cm^3
$c = 21.063$ (2) Å	$\mu = 19.8$ cm^{-1}
$\beta = 94.88$ (1)°	$V = 4728.4$ (9) Å^3
$R_F(F_o < 2.5\sigma) = 0.058$[a]	$R_w(F_o > 2.5\sigma) = 0.049$[b]
no corr for abs	

[a] $R(F_o) = \sum(F_o - F_c)/\sum(F_o)$. [b] $R_w(F_o) = [\sum(w(F_o - F_c)^2)/\sum(wF_o^2)]^{1/2}$.

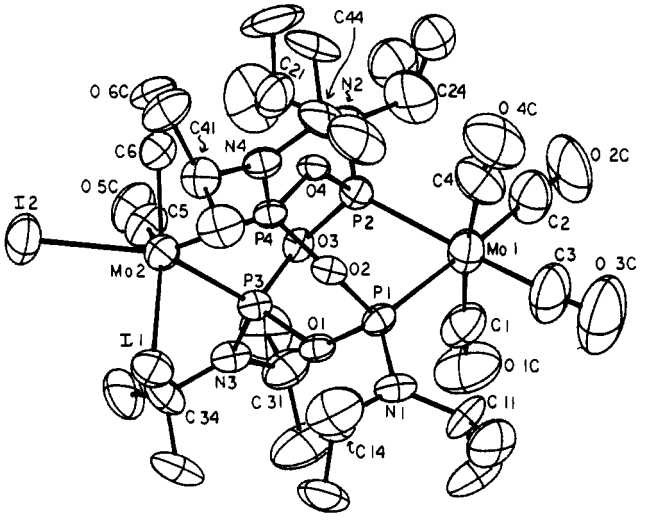

Figure 1. ORTEP drawing of $(CO)_4Mo[^iPr_2NPO]_4Mo(CO)_2I_2$ (3), showing 50% probability ellipsoids.

Molecular Structure of Complex 3. The molecular structure of $I_2(CO)_2Mo[^iPr_2NPO]_4Mo(CO)_4$ (3) is shown in Figure 1. Though the basic adamantanoid $Mo_2P_4O_4$ cage structure remains intact, the near D_{2d} symmetry of the parent compound has been substantially reduced.[8] Only an approximate mirror plane containing the atoms Mo(1), Mo(2), I(1), I(2), P(1), and P(2) remains, bisecting the molecule. The most interesting observation is the stereochemistry around the oxidized Mo(2) site. The six-coordinate metal coordination sphere approximates a trigonal prism (Figure 2) with the two trigonal faces defined by I(1), P(3), and P(4) and I(2) and the carbonyl oxygens O(5) and O(6), respectively. The I(1)–Mo(2)–I(2) angle of 85°, P(3)–Mo(2)–C(5) angle of 73°, P(4)–Mo(2)–C(6) angle of 74°, P(3)–Mo(2)–P(4) angle of 73°, and C(5)–Mo(2)–C(6) angle of 74° define the internal angles. The average Mo(2)–I distance is shortened at 2.744 (2) Å. Due to the nonoctahedral geometry at Mo(2), the diisopropylamino groups at the Mo(2) phosphorus atoms are bent toward the metal with an average Mo(2)–P–N angle of only 116° compared to the average Mo(1)–P–N angle of 127° at the unreacted $Mo(CO)_4$ site. The Mo–Mo separation remains essentially unchanged at 5.963 (2) Å compared to 6.001 (2) Å before iodination. At the unoxidized Mo(1), the distorted octahedral geometry of the parent complex is retained. The axial carbonyl carbon C(1) is tilted toward P(1) and away from P(2) by 8° while the other axial carbon C(4) is tilted toward P(2) by 4°. Due to the bending of N^iPr_2 groups toward Mo(1), compression of the ideally linear axial C(1)–Mo(1)–C(4) angle to 173° is actually less than that in the parent complex **1** (167°). Other bond distances and angles are not significantly altered.[8]

IR spectra of the complexes were examined with respect to two regions in particular. In the carbonyl region (near 2000 cm^{-1}), the position of the high-energy A_1 band [on the Mo(0)] provides a measure of the electron density at the metal.[10] In the dihalo complexes this band has moved to 2024 cm^{-1} (KBr) from its position at 2015 cm^{-1} in the parent complex, indicating a decrease in electron density at the Mo(0) atom transmitted from the ox-

Table VI. Bond Lengths (Å) and Angles (deg) for $Mo(CO)_2I_2[^iPr_2NPO]_4Mo(CO)_4$ (3)

Mo(1)–P(1)	2.491 (4)	P(3)–O(3)	1.64 (1)
Mo(1)–P(2)	2.481 (5)	P(3)–N(3)	1.63 (1)
Mo(1)–C(1)	2.01 (2)	P(4)–O(2)	1.62 (1)
Mo(1)–C(2)	2.02 (2)	P(4)–O(4)	1.623 (9)
Mo(1)–C(3)	1.95 (2)	P(4)–N(4)	1.65 (1)
Mo(1)–C(4)	2.04 (2)	N(1)–C(11)	1.47 (2)
Mo(2)–P(3)	2.448 (5)	N(1)–C(14)	1.52 (2)
Mo(2)–P(4)	2.440 (5)	N(2)–C(21)	1.50 (2)
Mo(2)–I(1)	2.752 (2)	N(2)–C(24)	1.54 (2)
Mo(2)–I(2)	2.737 (2)	N(3)–C(31)	1.53 (2)
Mo(2)–C(5)	1.92 (2)	N(3)–C(34)	1.50 (2)
Mo(2)–C(6)	1.96 (2)	N(4)–C(41)	1.52 (2)
P(1)–O(1)	1.67 (1)	N(4)–C(44)	1.50 (2)
P(1)–O(2)	1.64 (1)	C(1)–O(1C)	1.14 (2)
P(1)–N(1)	1.65 (1)	C(2)–O(2C)	1.12 (2)
P(2)–O(3)	1.66 (1)	C(3)–O(3C)	1.15 (3)
P(2)–O(4)	1.66 (1)	C(4)–O(4C)	1.11 (2)
P(2)–N(2)	1.65 (1)	C(5)–O(5C)	1.15 (2)
P(3)–O(1)	1.63 (1)	C(6)–O(6C)	1.14 (2)

P(1)–Mo(1)–P(2)	77.6 (1)	Mo(1)–C(3)–O(3C)	176.4 (2)
P(1)–Mo(1)–C(1)	87.8 (6)	Mo(1)–C(4)–O(4C)	173.1 (2)
P(1)–Mo(1)–C(2)	174.6 (6)	Mo(2)–C(5)–O(5C)	176.1 (2)
P(1)–Mo(1)–C(3)	99.9 (7)	Mo(2)–C(6)–O(6C)	176.9 (2)
P(1)–Mo(1)–C(4)	94.9 (6)	Mo(1)–P(1)–O(1)	111.1 (3)
P(2)–Mo(1)–C(1)	96.1 (6)	Mo(1)–P(1)–O(2)	112.7 (4)
P(2)–Mo(1)–C(2)	98.8 (6)	Mo(1)–P(1)–N(1)	125.5 (5)
P(2)–Mo(1)–C(3)	173.4 (8)	Mo(1)–P(2)–O(3)	114.3 (4)
P(2)–Mo(1)–C(4)	90.5 (6)	Mo(1)–P(2)–O(4)	110.0 (4)
C(1)–Mo(1)–C(2)	88.7 (9)	Mo(1)–P(2)–N(2)	127.9 (5)
C(1)–Mo(1)–C(3)	89.9 (1)	Mo(2)–P(3)–O(1)	120.0 (4)
C(1)–Mo(1)–C(4)	173.2 (9)	Mo(2)–P(3)–O(3)	110.2 (4)
C(2)–Mo(1)–C(3)	84.1 (9)	Mo(2)–P(3)–N(3)	116.0 (5)
C(2)–Mo(1)–C(4)	89.0 (9)	Mo(2)–P(4)–O(2)	120.0 (4)
C(3)–Mo(1)–C(4)	83.6 (1)	Mo(2)–P(4)–O(4)	111.6 (4)
I(1)–Mo(2)–I(2)	85.16 (5)	Mo(2)–P(4)–N(4)	115.0 (5)
I(1)–Mo(2)–P(3)	92.1 (1)	P(1)–O(1)–P(3)	130.6 (6)
I(1)–Mo(2)–P(4)	94.8 (1)	P(1)–O(2)–P(4)	129.8 (5)
I(1)–Mo(2)–C(5)	139.9 (5)	P(2)–O(3)–P(3)	127.6 (5)
I(1)–Mo(2)–C(6)	144.0 (5)	P(2)–O(4)–P(4)	129.2 (6)
I(2)–Mo(2)–P(3)	147.1 (1)	P(1)–N(1)–C(11)	118.8 (1)
I(2)–Mo(2)–P(4)	140.0 (1)	P(1)–N(1)–C(14)	116.2 (1)
I(2)–Mo(2)–C(5)	87.8 (5)	C(11)–N(1)–C(14)	124.6 (1)
I(2)–Mo(2)–C(6)	83.3 (5)	P(2)–N(2)–C(21)	120.0 (1)
P(3)–Mo(2)–P(4)	72.8 (1)	P(2)–N(2)–C(24)	120.0 (1)
P(3)–Mo(2)–C(5)	73.3 (5)	C(21)–N(2)–C(24)	124.1 (1)
P(3)–Mo(2)–C(6)	115.4 (5)	P(3)–N(3)–C(31)	114.9 (1)
P(4)–Mo(2)–C(5)	115.0 (6)	P(3)–N(3)–C(34)	117.1 (1)
P(4)–Mo(2)–C(6)	73.5 (5)	C(31)–N(3)–C(34)	127.1 (1)
C(5)–Mo(2)–C(6)	73.6 (7)	P(4)–N(4)–C(41)	115.1 (1)
Mo(1)–C(1)–O(1C)	174.3 (2)	P(4)–N(4)–C(44)	118.7 (1)
Mo(1)–C(2)–O(2C)	176.2 (2)	C(41)–N(4)–C(44)	124.5 (1)

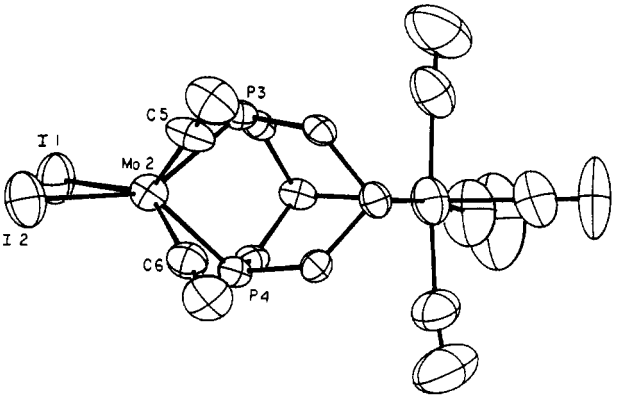

Figure 2. Partial ORTEP drawing of $(CO)_4Mo[^iPr_2NPO]_4Mo(CO)_2I_2$ (3), showing the trigonal-prismatic geometry about the oxidized metal center (50% probability ellipsoids).

(10) (a) Darensbourg, D. J.; Darensbourg, M. Y. *J. Chem. Educ.* **1970**, *47*, 33. (b) Darensbourg, D. J.; Darensbourg, M. Y. *J. Chem. Educ.* **1974**, *51*, 787.

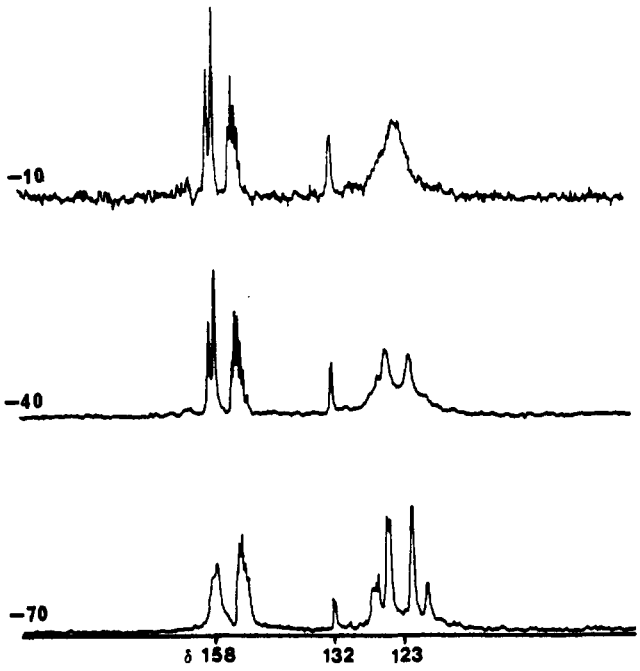

Figure 3. ^{31}P NMR spectra of the in situ reaction of **1** with I_2 to produce **9** at −70, −40, and −10 °C. The signal at 132 ppm results from the formation of small amounts of compound **3**.

idized Mo(II) site. A shift to higher energy, ranging from 10 to 19 cm^{-1}, is also observed for the P–O–P stretching vibrations in the dihalo complexes.

The oxidation of **1** with I_2 was attempted at low temperature to see if the saturated complex could be detected. Indeed, addition of 1 equiv of I_2 at 0 °C gave a product with a fluxional ^{31}P NMR spectrum, indicative of the seven-coordinate complex $I_2(CO)_3Mo[^iPr_2NPO]_4Mo(CO)_4$ (**9**). The broad signal at 123 ppm (due to the phosphorus atoms on the oxidized Mo) sharpens progressively as the temperature is lowered to −70 °C, where it begins to resemble an AA′BB′ pattern. Upon warming of the sample back to 0 °C, the original spectrum is first regenerated followed by loss of an additional CO to give **3** as the sample reaches room temperature (Figure 3).

This loss of CO is fully reversible. Addition of CO(g) to the sample regenerates the spectrum observed for **9**. Complex **3** will also add other ligands as evidenced by the reaction with acetonitrile. Treatment of the deep burgundy colored **3** with acetonitrile causes immediate precipitation of a bright yellow solid, which analyzes as expected for $(CH_3CN)I_2(CO)_2Mo[^iPr_2NPO]_4Mo(CO)_4$ (**10**). After 1 day under N_2, or several hours under vacuum, this solid loses CH_3CN and regains its original color and spectroscopic properties.

The success of the halide-exchange reaction and the isolation of the acetonitrile adduct **10** led us to believe that other coordinating solvents might also add to the vacant coordination site of the oxidized metal ions, possibly inducing the loss of halide ion. ^{31}P NMR spectroscopy showed this to be the case. Spectra of the dioxidized iodide complex **4** revealed regular changes (new resonances spread across the range δ 130–175 and reduction in the intensity of the original peaks) with increasing concentration of acetone-d_6 in $CDCl_3$ solution. This solvent-induced change in the ^{31}P NMR spectrum is observed with a variety of solvents. THF, ethyl acetate, 2,4-pentanedione, acetonitrile, and cyclopentanone also induced changes that were qualitatively similar to acetone but to varying degrees. All of these changes proved to be reversible upon removal of the solvent in vacuo, indicating that no loss of CO was involved.

Halogenation Reactions of $(CO)_4Mo[PhPO]_4Mo(CO)_4$. Halogenation of the phenyl-substituted compound $(CO)_4Mo[PhPO]_4Mo(CO)_4$ (**2**) was carried out in similar fashion. Elemental iodine or SO_2Cl_2 gave sequentially the dihalo $X_2(CO)_3Mo[PhPO]_4Mo(CO)_4$ (**11**, orange, X = I; **13**, yellow, X = Cl) and the tetrahalo $X_2(CO)_3Mo[PhPO]_4Mo(CO)_3X_2$ (**12**, orange, X = I; **14**, yellow, X = Cl) (Scheme III). The orange tetrabromo derivative (**15**) can be similarly prepared. These solid products are poorly characterized due to their propensity to decompose via CO loss to give dark oils. Only limited spectral and analytical data could, therefore, be obtained. The low-temperature ^{31}P NMR spectra of a mixture of the diiodo **11** and the tetraiodo **12** are shown in Figure 4. Multiplets assigned to complex **11** comprise an ABX_2 spin system with near coalescence of the upfield triplet at −70 °C. The broad singlet at δ 168 is assigned to complex **12**.

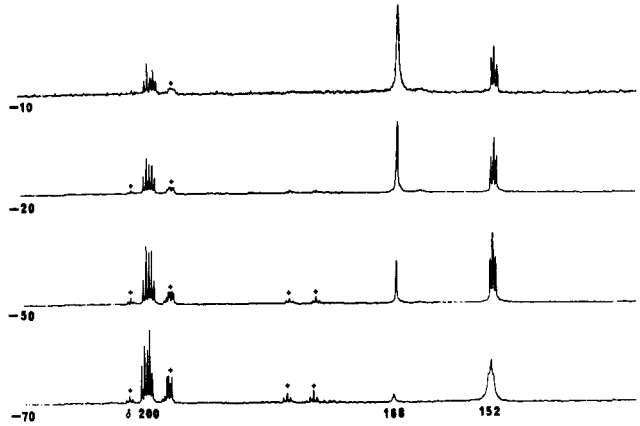

Figure 4. ^{31}P NMR spectra of $(CO)_4Mo[PhPO]_4Mo(CO)_3I_2$ (**11**) at −70, −50, −20, and −10 °C. The spectra were obtained by adding 1 mol of I_2/mol of **2** at −70 °C in CD_2Cl_2 and allowing the sample to warm to room temperature. Peaks marked "+" are impurities, most likely minor isomers of **11**. The singlet at δ 168 is due to **12**.

Scheme III

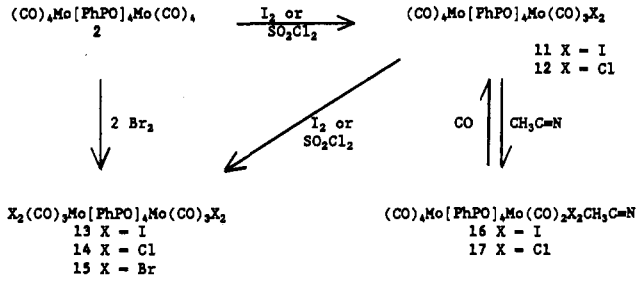

Table VII. Experimental Molecular Weights and Conductivites for **3–5**, **7**, and **8**

compd	MW[a] theory	MW[a] expt	molar[b] conductivity
3	1201.7	1234 ± 7	71
4	1399.5	1198 ± 27	89
5	1018.9	1010 ● 60	
7	1107.8	1169 ± 110	51
8			30

[a] Determined by vapor-pressure osmometry in $CHCl_3$. [b] In $dm^2/(\Omega$ mol) at 1.0×10^{-3} M in CH_3CN.

Complex **11** can be isolated as a stable acetonitrile adduct (yellow, **16**, Scheme III) upon addition of the solvent to solid **11**. This substitution is reversible as bubbling CO gas through a solution of **16** in CD_2Cl_2 regenerated **11**. Infrared data for **11–17** are presented in Table I.

Conductivity, Molecular Weight, and Magnetic Susceptibility. Conductivity measurements were made to determine the extent of ionization of **3**, **4**, **5**, **7**, and **8** in a coordinating solvent. The results are shown in Table VII. Typical values for 1:1 electrolytes at 1×10^{-3} M in acetonitrile are 120–160 Ω^{-1}, while those for a 1:2 electrolyte are near 260 Ω^{-1}.[11] It is clear from the experimental

(11) Geary, F. *Coord. Chem. Rev.* **1971**, *7*, 81–122.

data that these complexes do ionize in acetonitrile but only to a very moderate extent.

Molecular weight determinations were made via vapor-pressure osmometry in $CHCl_3$ solution for compounds **3–5** and **7**. The theoretical and experimental values are also given in Table VII. All complexes exist as monomeric species.

The magnetic susceptibilities of **3** and **4** were measured in an attempt to provide additional information about coordination geometry at the metal centers. However, the room temperature (25 °C) susceptibilities of **3** and **4** indicated the compounds were diamagnetic (-3.3×10^{-7} cgs and -4.0×10^{-7} cgs, respectively). The magnetic susceptibilities of **3** and **4** were also measured from 100 to 298 K. The values were the same as those obtained at room temperature within experimental error and exhibited no significant change over the temperature range, confirming the absence of any antiferromagnetic coupling.

Discussion

Halogenation Reactions of the Cage Complex 1. Halogenations of cage **1** proceeded readily at and below room temperature to give dihalo and tetrahalo products retaining the adamantanoid cage structure. Interestingly, when 1 mol equiv of iodine or sulfuryl chloride was used, essentially quantitative yields of the dihalo products **3** and **5** were obtained. If the two molybdenum centers in **1** were truly independent sites, the expected iodination result, for example, should have been a statistical mixture of 25% unreacted **1**, 50% **3**, and 25% **4**. This may be an indication of a cooperative effect between the cage metals, where oxidation at one site inhibits reaction at the second metal. Because of the large metal–metal separation of 5.96 Å in **3**, unmediated metal–metal interaction is unlikely and the P–O–P ligand bridges must be invoked in the relay of any such effects. Occurrence of two separate (irreversible) oxidation waves in the cyclic voltammogram of **1** appears consistent with this effect.[8] However, the opposite cooperativity observed for the bromination, with *no* observed formation of the mixed-valent dibromo complex **7** from 1 mol equiv of bromine, is puzzling. Evidence exists for the initial rapid formation of metal carbonyl/halogen adducts in kinetics studies of halogenation reactions before the actual electron transfer.[12] These contradictory observations may simply reflect different stabilities of the 1:1 versus the 2:1 halogen/cage adducts rather than actual cooperativity. Much remains to be done before the details of these processes can be elucidated.

Observation by NMR spectroscopy of the fluxional seven-coordinate $I_2(CO)_3Mo[^iPr_2NPO]_4Mo(CO)_4$ (**9**) at low temperature and its formation upon exposure of the six-coordinate complex **3** to a CO atmosphere confirm its intermediacy in the formation of **3**. The low affinity of **3** for CO and other Lewis bases is consistent with the enhanced stability of its 16-electron Mo(II) center. The presence of good π donors has been suggested as the origin of this phenomenon.[4b]

Halogenation Reactions of Cage Complex 2. Halogenations of the cage complex **2** with iodine or sulfuryl chloride also proceeded in a stepwise manner to give di- and tetrahalo products **11–14**. The tetrabromo derivative **15** has been prepared similarly. These are of much lower stability compared to cage **1** halogenation products **3–8**, rapidly losing CO and decomposing to ill-characterized oils upon standing for short periods of time. The formulation of the oxidized metal centers as being seven-coordinate $Mo(CO)_3X_2P_2$ is supported by the NMR and elemental analytical data.

The low-temperature ^{31}P NMR spectrum of **11** contains an upfield triplet at δ 152, which is near coalescence at −70 °C (Figure 4). This triplet can be assigned to the $Mo^{II}I_2$-site phosphorus atoms by analogy to complexes **3** and **9**. The apparent fluxionality at this site is consistent with the formation of a seven-coordinate $Mo(CO)_3X_2P_2$ coordination sphere as suggested for complex **9**. The reversible isolation of the acetonitrile adduct of **11**, **16**, also supports this formulation. The broad singlet (δ 168) resonance for the tetraiodo **12** also suggests the presence of fluxional seven-coordinate $Mo(CO)_3X_2P_2$ sites at both metal vertices. Elemental analyses further support this composition for complexes **12** and **15**.

The low stability and adoption of the higher coordination number in these halogenated derivatives compared to the cage **1** products are direct consequences of the very different steric and electronic environments provided by the P-phenyl substituent versus the diisopropylamino group. Unlike in **2**, substantial distortions from an idealized Mo coordination geometry are observed in parent cage **1** due to the four diisopropylamino groups. This is likely to destabilize a coordination number of 7 at the halogenated Mo(II) sites in **1** but not in **2**. A second significant factor should be the different ability of each substituent group to stabilize the 16-electron $Mo(CO)_2X_2P_2$ sites upon loss of the third CO. Competitive iodination between **1** and **2** clearly indicated a preference for oxidation of the former. This is consistent with the infrared as well as cyclic voltammetry data,[8] both indicating a more electron-rich metal center in **1** due to π donation of the amino nitrogens into the cage. The higher stability of the cage **1** halogenation products and their preference for the 16-electron six-coordinate Mo(II) sites compared to the cage **2** products can be similarly rationalized.

NMR Spectra. The ^{31}P NMR spectra for the Mo(II)/Mo(0) complexes **3**, **5**, and **7** show typical AMX_2 patterns. From the crystal structure of **3**, we can assign the X_2 portion of the spectrum to the two phosphorus atoms on the Mo(II) center. This agrees with the steady shifting of the X_2 resonance downfield with increasing electronegativity of the halide substituent. The minimal changes in the chemical shifts of the resonances on the unoxidized metal as a function of the halide ion are also in agreement with this assignment.

A series of heteronuclear NMR decoupling experiments were undertaken to assign more completely the individual spectra. The monoiodinated complex **3** was chosen for these studies on the basis of its solubility and well-resolved spectra. The ^1H NMR spectrum of **3** at room temperature in $CDCl_3$ solution exhibits two doublets of heptets, one each at 5.3 and 4.0 ppm, for the methine protons and four doublets, at 1.50, 1.38, 1.31, and 1.25 ppm, for the methyl groups. Single-frequency decoupling of the downfield methine caused collapse of the doublet at 1.50 ppm. Irradiation of the upfield methine signal rendered the remaining three methyl resonances singlets. The proton-coupled ^{31}P NMR spectrum of **3** shows two broad overlapping multiplets at 162 ppm, a doublet of quintets at 157 ppm, and a broad multiplet for the high-field resonance (132 ppm). Selective decoupling of the low-field methine proton caused collapse of the 157 ppm phosphorus signal to a doublet of triplets. Irradiation of the high-field methine protons rendered the phosphorus signals at 162 and 132 ppm doublets. Similarly, the doublet carbon resonance at 48.3 ppm has been correlated with the downfield methine proton and the triplet carbon resonance at 49.0 ppm and the two singlet carbon resonances at 47.0 and 48.0 ppm have been correlated with the upfield methine signal.

X-ray Structure of Complex 3. The adoption of the trigonal-prismatic geometry at the Mo(II) site in **3** has precedence in the reported structure of the $Mo(CO)_2[S_2CN^iPr_2]_2$ complex.[5a] Templeton and co-workers have shown that the combination of π-donor and -acceptor ligands can stabilize two of the octahedral metal-based t_{2g} orbitals while destabilizing the third in such a geometry.[4b] This accounts for the diamagnetism as well as the low electrophilicity of such 16-electron d^4 complexes. For complex **3**, the iodo ligands must serve adequately as π donors and the shortened Mo–I distance of 2.744 (2) Å (compared to 2.86 Å in $Mo(CO)_3I_2(Ph_2POPPh_2)$, e.g.) certainly supports this premise.[7a] The acute carbonyl–Mo–carbonyl angle of 74° is also consistent with similarly compressed angles in $Mo(CO)_2[S_2CN^iPr_2]_2$ of 74° and $Mo(CO)_2Py_2(O\text{-}^tBu)_2$ of 72° in order to optimize metal-to-CO π bonding.[4b] The readily reversible association of various Lewis bases with **3** is further manifestation of its attenuated electron deficiency. Our EHMO calculations using $Mo(CO)_2Cl_2[P(OH)_2NH_2]_2$ as a model revealed a 1.58-eV HOMO/LUMO gap for the trigonal-prismatic geometry and only a 0.25 eV gap

(12) Kramer, G.; Poe, A.; Amer, S. *Inorg. Chem.* **1981**, *20*, 1362.

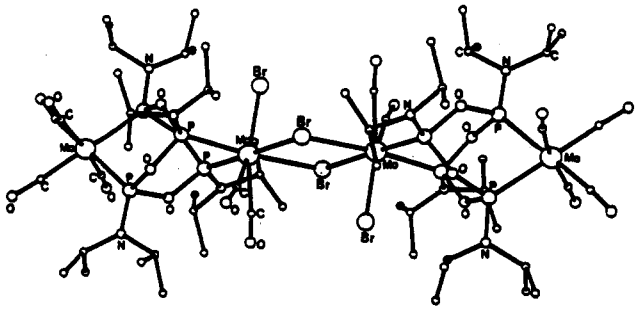

Figure 5. Drawing of the molecular structure of the dimer $[(CO)_4Mo[^iPr_2NPO]_4Mo(CO)_2Br_2]_2$ (**7**).

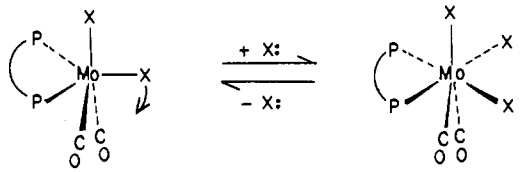

Figure 6. Geometric changes required about the oxidized metal atom in the dimerization of $(CO)_4Mo[^iPr_2NPO]_4Mo(CO)_2Br_2$ (**7**).

for the octahedral one,[13] a result qualitatively similar to the previously reported HOMO/LUMO gaps (1.21 and 0.20 eV, respectively) of the model $Mo(CO)_2(S_2CNH_2)_2$ complex.[14]

We have also completed a structural study on crystals of the dibromo complex **7** grown from acetonitrile. Unfortunately, crystal decomposition and packing disorder curtailed full refinement and thus a detailed presentation of the structural data is not warranted.[15] Nevertheless, the overall molecular geometry and metal coordination spheres are clearly revealed (Figure 5). It is a dimeric structure wherein two cage molecules are linked via two bromide bridges at the respective Mo(II) sites. Of particular interest is the seven-coordinate geometry at these sites which approximates a capped trigonal prism with a third bromide capping the rectangular face generated from the two bridging bromides and two cage phosphorus atoms. Only minimal distortions from the six-coordinate trigonal prismatic geometry of the Mo(II) in complex **3** are needed to accommodate a seventh bridging halide ligand and form this dimeric structure (Figure 6). We believe the better donor ability of the bromide compared to the iodide to be responsible for this change in solid-state structure. In solution, both **3** and **7** are monomeric and gave similar spectra, consistent with the solid-state geometry of complex **3**.

In summary, the following conclusions have been drawn. (1) The cage complex **1**, $(CO)_4Mo[^iPr_2NPO]_4Mo(CO)_4$, is readily halogenated to give mixed-valent dihalo and tetrahalo derivatives. (2) Spectroscopic and structural data confirm retention of the parent $Mo_2P_4O_4$ cage structure and adoption of a trigonal-prismatic stereochemistry at the six-coordinate Mo(II) sites. (3) Upon halogenation, the phenyl-substituted $(CO)_4Mo[PhPO]_4Mo(CO)_4$ cage (**2**) gave relatively unstable dihalo and tetrahalo derivatives which may contain seven-coordinate Mo(II) centers. (4) Cage complex **1** is selectively halogenated in preference to cage **2**. (5) The stability and stereochemistry of cage **1** halogenation products arise from a combination of steric and electronic factors due to its $^iPr_2N$ substituents.

Experimental Section

All synthetic procedures were carried out using standard Schlenk technique under argon or nitrogen atmosphere. Toluene was purified by distillation from sodium metal. Dichloromethane and hexanes were distilled from CaH_2. Ether and THF were distilled from Na/benzophenone ketyl. PCl_3, $PhPCl_2$, and $Mo(CO)_6$ were purchased from Alfa Products and used without further purification. IR spectra were recorded on a Perkin-Elmer 283B spectrophotometer and were calibrated against polystyrene.[16] NMR spectra were recorded on a JEOL FX-90Q or a Bruker AM360 instrument and calibrated against TMS (^1H), solvent (^{13}C), and external 85% H_3PO_4 or Ph_3P (^{31}P). Spectra were obtained in $CDCl_3$ solution unless otherwise noted in Tables II–IV. ^{13}C and ^{31}P NMR spectra are broad-band proton decoupled unless otherwise noted. Room-temperature magnetic moments were measured on a Johnson Matthey magnetic susceptibility balance. Variable-temperature magnetic moments were measured on a vibrating-sample magnetometer with modified cryostat[17] over the temperature range 96 K to room temperature. Molecular weight measurements were carried out using a Microlabe V/P/O Model 301A vapor-pressure osmometer. Elemental analyses were performed by the University Instrumentation Center, Parsons Hall, University of New Hampshire, Durham, NH. The syntheses of **1** and **2** have been previously reported.[8]

$I_2(CO)_2Mo[^iPr_2NPO]_4Mo(CO)_4$ (3). A solution of I_2 in CH_2Cl_2 (5.58 mL of 0.0249 g/mL, 0.139 g) was added with stirring to a solution of **1** (0.50 g, 0.50 mmol) in 10 mL of CH_2Cl_2. The solution turned brown and then dark red. After 1 h the solvent was removed in vacuo to yield a burgundy powder. Acetonitrile (5 mL) was added and the resulting bright yellow powder collected by suction filtration and dried under vacuum to give a burgundy-colored solid, 0.53 g (89%). IR (KBr): 2025, 1980, 1915 b (CO), 892, 885 cm^{-1} (P–O–P). ^{31}P NMR: δ 161.8 (d of t, J_d = 39.9 Hz, J_t = 2 Hz), 155.4 (d of t, J_2 = 39.9 Hz, J_3 = 11.7 Hz), 132.7 (d of d, J = 11.7 and 2 Hz). ^1H NMR: δ 5.3 (hept, J = 7 Hz, 1 H), 4.05 (hept, J = 7 Hz, 3 H), 1.35 (24 H). ^{13}C NMR: δ 233.4 (t, J = 27 Hz), 213.0 (d of d, J = 10 and 4 Hz), 211.0 (t, J = 15 Hz), 206.2 (t, J = 12 Hz), 49.0 (t, J = 4 Hz), 48.3 (d, J = 8 Hz), 48.0 (s), 47.0 (s), 24.5 (d, J = 2 Hz), 24.0 (d, J = 2 Hz), 23.2 (s). Anal. Calcd for $C_{30}H_{56}I_2Mo_2N_4O_{10}P_4$: C, 29.97; H, 4.69; N, 4.66. Found: C, 29.82; H, 4.81; N, 4.63.

$I_2(CO)_2Mo[^iPr_2NPO]_4Mo(CO)_2I_2$ (4). A solution of I_2 in CH_2Cl_2 (10.6 mL, 0.020 g/mL, 0.837 mmol) was added with stirring to a solution of **1** (0.42 g, 0.42 mmol) in 10 mL of CH_2Cl_2. The solution turned brown and then dark red. After 1 h the solvent was removed in vacuo to yield a burgundy-colored powder. Hexanes (5 mL) were added, and the solid was collected by suction filtration and dried under vacuum to yield a burgundy powder, 0.56 g (91%). IR (KBr): 2045 w, 1983, 1968, 1922, 1911 (CO), 885 cm^{-1} (P–O–P). ^{31}P NMR: AA'BB' pattern at 38 MHz; δ 144.7, 137.2 (J_{app} = 157 and 3 Hz); at 146 MHz AB pattern only (J_{app} = 157). ^1H NMR: δ 4.9 (m, 1 H), 3.75 (m, 1 H), 1.40 (approximate quartet, 12 H). ^{13}C NMR: δ 231.1, 229.5 (two d of d, J = 11 and 41 Hz), 50.6 (d, J = 8 Hz), 49.7 (d, 8 H), 24.6 (s), 23.1 (m). Anal. Calcd for $C_{28}H_{56}I_4Mo_2N_4O_8P_4$: C, 24.02; H, 4.03; N, 4.00. Found: C, 23.96; H, 4.12; N, 3.94.

$Cl_2(CO)_2Mo[^iPr_2NPO]_4Mo(CO)_4$ (5). SO_2Cl_2 (0.80 mL, 0.31 mmol) was added slowly with vigorous stirring to a solution of **1** (0.310 g, 0.309 mmol) in 5 mL of CH_2Cl_2. After 1 h, a small amount of bright yellow precipitate (**6**) had formed. The precipitate was removed by filtration, and hexane (3 mL) was added slowly to the filtrate with stirring. The resulting bright yellow solid was collected by suction filtration and dried under vacuum to yield 0.27 g (85%). IR (KBr): 2025, 1975, 1960, 1920 (CO), 885 cm^{-1} (P–O–P). ^{31}P NMR: δ 162.9 (d, J = 39 Hz), 157.5 (d of t, J_2 = 39, J_3 = 15 Hz), 152 (d, J = 15 Hz). ^1H NMR: δ 5.12 (m, 1 H, NCH), 4.18 (m, 2 H, NCH), 3.92 (m, 1 H, NCH), 1.46, 1.39, 1.34 (three d, ratio = 1:2:1, J = 7 Hz, 24 H, CH_3's). ^{13}C NMR: δ 239.5 (t, J = 27 Hz), 212.8 (t, J = 9 Hz), 212.1 (t, J = 12 Hz), 206.9 (t, J = 11 Hz), 49.5 (t, J = 12 Hz), 48.0 (d, J = 7 Hz), 47.7 (s), 24.7, 24.5, 24.0, 23.3 (four s). Anal. Calcd for $C_{30}H_{56}Cl_2Mo_2N_4O_{10}P_4$: C, 35.34; H, 5.54; N, 5.50. Found: C, 34.33; H, 5.50; N, 5.50. Attempts to purify the material by recrystallization were unsuccessful.

$Cl_2(CO)_2Mo[^iPr_2NPO]_4Mo(CO)_2Cl_2$ (6). SO_2Cl_2 (1.50 mL, 0.565 mmol) was added slowly with vigorous stirring to a solution of **1** (0.310 g, 0.309 mmol) in 10 mL of CH_2Cl_2, giving a yellow solution. After 1 h, a bright yellow precipitate had formed. The precipitate was collected by suction filtration and dried under vacuum to yield a bright yellow powder, 0.29 g (99%). IR (KBr): 1979, 1929 (CO), 897 cm^{-1} (P–O–P). Anal. Calcd for $C_{28}H_{56}Cl_4Mo_2N_4O_8P_4$: C, 32.51; H, 5.46; N, 5.42. Found: C, 32.96; H, 5.42; N, 5.42.

$Br_2(CO)_2Mo[^iPr_2NPO]_4Mo(CO)_4$ (7). Et_4NBr (0.0662 g, 0.314 mmol) was added to a stirred solution of **3** (0.1891 g, 0.157 mmol) in 9

(13) Calculations were performed using the EHMO method of Hoffmann (Hoffmann, R. *J. Chem. Phys.* **1963**, *39*, 1397). Program QCPE 358 from the Quantum Chemistry Program Exchange was used. Parameters employed were as listed in ref 4b.

(14) Templeton, J. L.; Winston, R.; Ward, B. *J. Am. Chem. Soc.* **1981**, *103*, 7713.

(15) The crystallographic data obtained for **7** are available as supplementary material.

(16) IR spectra of solids were recorded in a KBr matrix. The possibility exists for halide exchange with compounds containing iodide or chloride. We do not believe this occurs to a significant extent in these systems on the basis of the reproducibility of spectra for each compound.

(17) Landee, C. P.; Greeney, R. E.; Lamas, A. C. *Rev. Sci. Instrum.* **1987**, *58*, 39–40.

mL of 2:1 CH_2Cl_2/CH_3CN. The mixture was stirred for 1 h and the solvent removed under vacuum. Toluene (5 mL) was added and the mixture stirred for 5 min. A white precipitate of Et_4NI was removed by filtration and the toluene removed from the filtrate under vacuum to yield an orange solid. The solid was washed with hexane to remove unreacted **3**, and the resulting yellow powder was dried under vacuum to give 0.13 g (76%). IR (KBr): 2026, 1972, 1958, 1923 b (CO), 880 cm^{-1} (P–O–P). ^{31}P NMR: δ 162.9 (d, J = 40 Hz), 157.5 (d of t, J_2 = 40, J_3 = 15 Hz), 147.1 (d, J = 15 Hz). ^1H NMR: δ 5.3 (hept, 1 H, J = 7 Hz), 4.10 (hept, 3 H, J = 7 Hz), 1.35 (m, 5 lines, 24 H). ^{13}C NMR: δ 236.0 (t, J = 31 Hz), 212.8 (d of d, J = 13, 4 Hz), 212.2 (t, J = 13 Hz), 206.3 (t, J = 12 Hz), 49.9, 48.7, 47.5 (three s), 48.0 (d, J = 4 Hz), 24.6 (s), 24.1 (s), 23.43 (t, J = 4 Hz). Anal. Calcd for $C_{30}H_{56}Br_2Mo_2N_4O_{10}P_4$: C, 32.51; H, 5.09; N, 5.05. Found: C, 32.36; H, 5.44; N, 4.91.

$Br_2(CO)_2Mo[^iPr_2NPO]_4Mo(CO)_2Br_2$ (8). A solution of Br_2 in CH_2Cl_2 (7.20 mL, 0.020 g/mL, 0.88 mmol, 5% excess) was added with stirring to a solution of **1** (0.42 g, 0.42 mmol) in 10 mL of CH_2Cl_2 resulting in a red-orange solution. After 1 h, the solution had turned deep red and a yellow precipitate formed. The solvent was reduced to 5 mL under vacuum and hexane (5 mL) was added. The bright yellow solid was collected by suction filtration and dried under vacuum to give 0.52 g (95%). IR (KBr): 1979, 1920 (CO), 890 cm^{-1} (P–O–P). ^{31}P NMR: AA′BB′ pattern; δ 157.9, 145.1 (two d of d, J_{app} = 24 and 107 Hz). ^1H NMR: δ 4.9 (m, 1 H), 3.75 (m, 1 H), 1.40 (approximate quartet, 12 H). ^{13}C NMR: δ 230.4 (m), 49.3 (m), 24.8 (s), 23.2 (m). Anal. Calcd for $C_{28}H_{56}Br_4Mo_2N_4O_8P_4$: C, 27.74; H, 4.66; N, 4.58. Found: C, 27.33; H, 4.68; N, 4.56.

$(CH_3CN)I_2(CO)_2Mo[^iPr_2NPO]_4Mo(CO)_4$ (10). Compound **3** (0.25 g, 0.21 mmol) was triturated with acetonitrile (5 mL) for 2 h. The resulting bright yellow solid was collected by filtration and dried under a stream of N_2 to give 0.24 g (92%). Compound **10** loses acetonitrile slowly under inert atmosphere or rapidly under vacuum. NMR spectra were not obtained; the compound is insoluble in CD_3CN and loses the acetonitrile ligand in other solvents. IR (solid): 2344 (C≡N), 2025, 1990, 1980, 1932, 1920, 1908 (C≡O), 897, 882 cm^{-1} (POP). Anal. Calcd for $C_{32}H_{59}I_2Mo_2N_5O_{10}P_4$: C, 30.91; H, 4.78; N, 5.63. Found: C, 30.58; H, 4.66; N, 5.43.

$I_2(CO)_3Mo[PhPO]_4Mo(CO)_3I_2$ (12). Compound **2** (0.3465 g, 0.380 mmol) was dissolved in CH_2Cl_2 (10 mL), and the solution was cooled to 0 °C. I_2 (0.1929 g, 0.760 mmol) was added with vigorous stirring and the mixture cooled to −10 °C. After 0.5 h, the solvent was removed under vacuum and the residue was washed with cold hexane (10 mL). The resulting yellow solid was collected by filtration and dried under vacuum to yield 0.330 g (78%). IR (KBr): 1992, 1931, 1883 (CO), 911 cm^{-1} (P–O–P). ^{31}P NMR: broad resonance at 168 ppm observed at −40 °C. Anal. Calcd for $C_{30}H_{20}I_4Mo_2O_{10}P_4$: C, 26.40; H, 1.47. Found: C, 26.44; H, 1.95.

$Cl_2(CO)_3Mo[PhPO]_4Mo(CO)_3Cl_2$ (14). Compound **2** (0.1676 g, 0.184 mmol) was dissolved in CH_2Cl_2 (5 mL). SO_2Cl_2 (0.90 mL, 0.37 mmol) was added with vigorous stirring, producing an orange solution, and the mixture cooled to −5 °C. After 1 h, the solvent was reduced by half and cold hexane (2 mL) added slowly via syringe. The resulting yellow solid was collected by filtration and dried under vacuum to yield 0.129 g (70%). IR (KBr): 1978, 1917 (CO), 902 cm^{-1} (P–O–P). Anal. Calcd for $C_{30}H_{20}Cl_4Mo_2O_{10}P_4$: C, 36.07; H, 2.00. Found: C, 35.17; H, 2.42.

$Br_2(CO)_3Mo[PhPO]_4Mo(CO)_3Br_2$ (15). Compound **2** (0.3120 g, 0.3520 mmol) was dissolved in CH_2Cl_2 (5 mL) and Br_2 (1.1 mL of a solution of Br_2 in CH_2Cl_2, 0.739 mmol) was added dropwise via syringe with vigorous stirring to produce an orange solution. After 1 h, an orange precipitate had formed, which was removed by filtration and dried under vacuum. Cold hexane (3 mL) was added to the filtrate, and an orange precipitate formed, which was collected by filtration and dried under vacuum. Microanalysis showed the two solids to have the same composition, the combined yield was 0.2931 g (70%). IR (KBr): 1988, 1931, 1883 (CO), 900 cm^{-1} (P–O–P). Anal. Calcd for $C_{30}H_{20}Br_4Mo_2O_{10}P_4$: C, 30.61; H, 1.79. Found: C, 30.61; H, 1.96.

$(CH_3CN)I_2(CO)_2Mo[PhPO]_4Mo(CO)_4$ (16). Compound **2** (0.2673 g, 0.2930 mmol) was dissolved in CH_2Cl_2 (10 mL) and cooled to 0 °C. I_2 (0.0744 g, 0.2930 mmol) was added with vigorous stirring and the mixture cooled to −10 °C. The progress of the reaction may be conveniently monitored by IR spectroscopy. After 0.5 h, IR spectroscopy showed the absence of starting material and the solvent was removed under vacuum. The residue was washed with cold acetonitrile (4 mL), and the resulting yellow solid was collected by filtration and dried under vacuum to yield 0.221 g (64%). IR (KBr): 2040, 1998, 1936, 1916 (CO), 902 cm^{-1} (P–O–P). Anal. Calcd for $C_{32}H_{23}I_2Mo_2NO_{10}P_4$: C, 33.39; H, 2.01; N, 1.22. Found: C, 33.64; H, 2.07; N, 1.23.

$(CH_3CN)Cl_2(CO)_2Mo[PhPO]_4Mo(CO)_4$ (17). Compound **2** (0.155 g, 0.170 mmol) was dissolved in CH_2Cl_2, and the solution was cooled to −5 °C. Sulfuryl chloride (0.41 mL, 0.17 mmol) was added dropwise via syringe with vigorous stirring, producing an orange solution and abundant gas evolution. After 0.5 h, a small amount of yellow solid appeared (compound **14**) and was removed by filtration. Cold acetonitrile (1 mL) was added to the filtrate, and the mixture was cooled to −40 °C. A bright yellow powder formed, which was collected by filtration and dried to yield 0.124 g (77%). IR (KBr): 2035, 1973, 1936 (CO), 897 cm^{-1} (P–O–P). This compound readily loses the acetonitrile ligand and decomposes. Several attempts at microanalysis were unsuccessful.

X-ray Structural Determination of Complex 3. Crystals of **3** were grown from hexane, and a 0.20 × 0.20 × 0.30 mm sample was mounted on a goniometer head for data collection on a Nonius CAD-4 diffractometer. A total of 13 845 reflections were measured with 6113 of these unique, and 4029 were considered significant using the $2.5\sigma(I_{net})$ criterion. The structure was solved using MULTAN.[18] All atoms were refined anisotropically except C(25) and C(26), which were disordered and were given half-occupancies along with C(25′) and C(26′). Details of the data collection are listed in Table V. All computations were carried out on the NRC-VAX PDP-81 system of programs adapted for the VAX 11/780 computer.[19] Full atomic coordinates and anisotropic thermal parameters plus structure factor tables are included in the supplementary material.

Acknowledgment. We wish to thank Wan-ru Zhang for her assistance in obtaining the temperature-dependent magnetic susceptibility data. Financial assistance from the Petroleum Research Fund, administered by the American Chemical Society, is gratefully acknowledged.

Registry No. **1**, 88008-34-8; **2**, 117339-95-4; **3**, 137917-40-9; **4**, 137917-41-0; **5**, 137917-42-1; **6**, 137917-43-2; **7**, 137917-44-3; **8**, 137917-45-4; **9**, 137917-46-5; **10**, 137917-47-6; **11**, 137917-48-7; **12**, 137917-49-8; **13**, 137917-50-1; **14**, 137917-51-2; **15**, 137917-52-3; **16**, 137917-53-4; **17**, 137917-54-5.

Supplementary Material Available: Complete listings of refined atomic coordinates and thermal parameters for compound **3** and listings of crystal data, approximate atomic coordinates and thermal parameters, and approximate bond distances and angles and an atom-numbering figure for compound **7** (7 pages); listings of calculated and observed structure factors for **3** and **7** (56 pages). Ordering information is given on any current masthead page.

(18) Germain, G.; Main, P.; Woolfson, M. M. *Acta Crystallogr.* **1971**, *A27*, 368.

(19) (a) Grant, D. F.; Gabe, E. J. *J. Appl. Crystallogr.* **1978**, *11*, 114. (b) LePage, Y.; Gabe, E. J.; Calvert, L. D. *J. Appl. Crystallogr.* **1979**, *12*, 25. (c) Larson, A. C.; Gabe, E. J. *Computing in Crystallography*; Delft University Press: Delft, Holland, 1978; p 81.